Biomedical Signal Processing and Control 108 (2025) 107894

Contents lists available at ScienceDirect

Biomedical Signal Processing and Control

journal homepage: www.elsevier.com/locate/bspc

Enhancing user experience in c-VEP-based BCI: Effects of visual stimulus opacity on performance and visual fatigue

Ana Martín-Fernández [a,*], Víctor Martínez-Cagigal [a,b], Selene Moreno-Calderón [a], Eduardo Santamaría-Vázquez [a,b], Roberto Hornero [a,b]

[a] Grupo de Ingeniería Biomédica (GIB), Universidad de Valladolid, Paseo de Belén, 15, Valladolid, 470011, Castilla y León, Spain
[b] Centro de Investigación Biomédica en Red en Bioingeniería, Biomateriales y Nanomedicina (CIBER-BBN), Spain

ARTICLE INFO

Keywords:
Brain-computer interfaces (BCI)
Code-modulated visual evoked potentials (c-VEP)
Opacity
Visual fatigue

ABSTRACT

Brain-computer interfaces (BCI) based on code-modulated visual evoked potentials (c-VEP) enable users to control devices through brain activity. These systems typically employ black and white flashes encoded via pseudo-random binary sequences to synchronize brain responses with specific commands. However, this traditional encoding often induces visual fatigue in users. Additionally, the sharp contrast of black and white commands can obscure the background on which they are displayed, complicating the integration of this technology in dynamic environments. Using semi-transparent stimuli could address these issues by reducing eyestrain and enabling compatibility with diverse backgrounds. However, the impact of opacity in c-VEP stimuli remains unexplored. This study aims to assess how varying visual stimulus opacity influences system accuracy and user experience. Six different opacity and background combinations were tested with ten healthy participants, who rated visual fatigue on a scale from 0 (none) to 10 (extreme) after each condition. Results showed that traditional encoding achieved 100% accuracy but induced high fatigue (6.4 points). A configuration with 100% opacity for black and 50% for white maintained high accuracy (99.38%) while reducing fatigue to 3.7 points. Brain responses were consistent when both black and white stimuli were present, but patterns changed when one color was omitted. Spatial filters revealed stable c-VEP decoding from the parieto-occipital cortex, with slightly higher activation in low-contrast conditions. The findings from this study suggest that adjusting the opacity of stimuli in c-VEP-based BCI can optimize the balance between performance and user experience. Implementing a reduction in opacity not only improves visual fatigue but may also facilitate the integration of c-VEP systems into lifelike environments.

1. Introduction

Brain-computer interfaces (BCI) enable online interaction with the environment through decodification of brain signals [1]. This technology could have particular relevance in several fields, including inducing neuroplasticity in the rehabilitation context [2], contributing to the video game industry [3] and assisting motor-impaired patients (e.g., wheelchair control, alternative communication, etc.) [4]. Typically, brain activity is recorded using electroencephalography (EEG) due to its non-invasive nature, portability, and cost-effectiveness compared to other methods [5]. Signal processing algorithms are then applied to EEG signals to extract and classify features that help to identify user intentions. Finally, these intentions are translated into specific actions by the system. However, it is important to note that EEG signals alone do not literally translate user thoughts into command execution; rather, measurable neural activity changes (i.e., control signals) are needed to decode user intentions [1].

Among the various control signals used in BCI, code-modulated visual evoked potentials (c-VEP) have recently emerged in the literature as a promising alternative for developing fast and accurate systems [6]. These BCI have demonstrated the ability to achieve accuracies exceeding 90%, with calibration times ranging from one to five minutes and selection times between one and five seconds per command [7–9]. These potentials are voltage changes in the EEG signal produced in response to external pseudo-random visual stimulation. Typically, visual stimulation is presented to the user as a series of black and white flashes that blink according to a pseudo-random binary sequence. When the user focuses on a flashing command, brain activity responds in a distinctive manner that is related to the sequence encoding the observed command. This allows the system to determine where the

* Corresponding author.
E-mail address: ana.martin.fernandez23@uva.es (A. Martín-Fernández).

https://doi.org/10.1016/j.bspc.2025.107894
Received 25 November 2024; Received in revised form 4 March 2025; Accepted 14 April 2025
Available online 30 April 2025

user is looking at and execute different commands accordingly. Furthermore, this approach enables the encoding of multiple commands through various sequences or shifted versions of the same sequence, effectively increasing the range of commands that can be executed in response to user attention [6].

Despite the promising results of c-VEP, they also present some limitations. A significant drawback is the visual fatigue experienced by users during prolonged exposure to the flashing stimuli [10]. The high contrast between the black and white flickering patterns can lead to eyestrain and discomfort, which not only impacts users physically but also affects their ability to concentrate and stay engaged. Furthermore, the traditional black and white coding of c-VEP commands poses a challenge for integrating this technology within dynamic environments. The opaque nature of these flashes can obscure background details, which is particularly problematic in settings where users need to maintain awareness of the environment, such as when BCI are combined with extended reality (XR) technologies.

Studies in scientific literature have approached user visual fatigue in various ways. One well-established solution is using monitors with higher refresh rates for c-VEP display. Conventional screens typically operate at 60 Hz, but several studies show that increasing the refresh rate to 120 Hz reduces visual fatigue while allowing for faster selections [11–13]. Another research area focuses on the generation pseudo-random codes. Typically, maximum-length sequences (m-sequences) are employed. However, studies such as those by Shirzhiyan et al. (2019) [14], Castillos et al. (2023) [9] and Lai et al. (2024) [15] suggest alternative sequences that concentrate most of their power in higher frequencies, which has been demonstrated to reduce visual fatigue. Additionally, non-binary m-sequences that shift across a broader gray scale range, instead of traditional black and white encoding, have been shown to improve user experience [13,16]. Lastly, recent research by Fernández-Rodríguez et al. (2023) [17] found that some variations of spatial frequency in checkerboard-like stimuli (e.g., 16×16 squares per stimulus) are also effective in minimizing visual fatigue.

Currently, there are no studies in the literature exploring the integration of c-VEP-based BCI into realistic environments, nor how presentation of visual stimuli might influence such integration. However, research on other control signals, such as steady-state visual evoked potentials (SSVEP), has approached this integration through combination of BCI with XR technologies [18,19]. In SSVEP-based BCI combined with XR, some studies have investigated how different aspects of visual stimuli may influence technology performance. For example, Du and Zhao (2022) [20] examined the effect of stimulus colors on SSVEP-based BCI in augmented reality, or Zehra et al. (2023) [21] evaluated various stimuli based on size and brightness levels. Additionally, Liu et al. (2024) [22] explored the effects of 2D versus 3D stimuli, including a 3D-blink condition where flickering stimuli were presented as white-transparent, completely omitting the black stimulus. Their research found that accuracy decreased from 86.17% in the 3D condition to less than 80% in the 3D-blink condition. However, participants reported the 3D-blink condition as more comfortable [22]. Although these results are intriguing, there is a lack of a comprehensive analysis regarding how completely making one stimulus transparent affects both system performance and brain response.

Opacity, in the context of visual stimuli, refers to the degree to which an element prevents visibility through it. Adjusting opacity from visual stimuli could offer an innovative solution to some of the challenges faced by c-VEP-based BCI. On the one hand, using semi-transparent stimuli would reduce the contrast of flickering stimuli, which could alleviate visual fatigue. On the other hand, semi-transparency would allow for better background visibility, which could be beneficial for integrating c-VEP-based BCI into lifelike environments. Despite the various attempts to enhance user experience and achieve practical BCI, there are still no studies in the scientific literature that have examined the effect of stimulus opacity on c-VEP-based BCI performance and user experience, nor how this factor could facilitate integration with dynamic environments by allowing commands to be superimposed on realistic scenarios without obscuring content. The key innovations proposed in this study are: (i) introducing a degree of transparency to c-VEP commands and (ii) integrating commands into a lifelike background. This raises two central questions: (1) is there a relationship between variations in visual stimulus opacity and c-VEP decoding performance, and (2) do these opacity variations affect user experience, particularly in terms of visual fatigue? Thus, the main objective of this study lies in answering these questions by analyzing how stimulus opacity influences both system performance and user experience in c-VEP-based BCI.

2. Methods

2.1. Participants

A total of 10 healthy participants were recruited to participate in the study, with a mean age of 26.70 ± 4.80 years. Among them, 6 were male and 4 were female. All participants had normal or corrected to normal vision. Prior to the experiment, all of them were informed about the purpose of the study, the possible risks, and the experimental protocol to be performed. All participants gave informed consent.

2.2. Signals

For EEG signal recording, a *g.USBamp* amplifier (g.Tec, *Guger Technologies*, Graz, Austria) was used. The equipment had a sampling frequency of 256 Hz and 16 active electrodes (F3, Fz, F4, C3, Cz, C4, CPz, P3, Pz, P4, PO7, POz, PO8, Oz, I1, I2) placed on the scalp according to the International 10-10 System [23]. The ground electrode was positioned at AFz, while the common reference was placed at the right earlobe (A2). The equipment was connected to an Intel Core i7-13700 PC with 32 GB of RAM. MEDUSA© [24] was employed to monitor the data via the lab streaming layer protocol [25], as well as to run the application and perform online signal processing. The application was displayed on a Full HD 144 Hz LED monitor, which was capable of presenting the c-VEP sequence at a sampling rate of 120 Hz.

2.3. Code generation

In this research, the sequence used to encode visual stimuli was an m-sequence. M-sequences are among the most commonly used pseudo-random sequences in c-VEP-based BCI [6]. These binary sequences exhibit a flat autocorrelation profile, with value 1 for unshifted version of the sequence and $-1/N$ for shifted versions of the sequence, where N is the length of the m-sequence [26]. This allows multiple commands to be encoded using a single sequence and its temporally shifted versions, following the circular shifting paradigm [6]. As a result, the calibration time is drastically reduced, as there is no need to calibrate the system for each command individually. Instead, the brain response to the original version of the sequence is computed, and templates for the remaining commands are derived by temporally shifting the signal [6].

This type of sequence can be generated using a linear feedback shift register (LFSR) [27]. A shift register is a logic circuit consisting of a series of cascaded flip-flops (states), where the output of each flip-flop is connected to the input of the next. In an LFSR, the input bit is determined by a linear transformation of two or more bits within the register. With each clock signal, the bits shift through the states. The output from an LFSR can be made pseudo-random by appropriately initializing the states with a seed different from a zero vector and using a primitive feedback polynomial. This process generates m-sequences of length $N = 2^m - 1$ [28].

The LFSR used to generate the m-sequence for this study contained six states, resulting in an m-sequence of 63 bits ($N = 2^6 - 1$). The seed used to initialize the states is ($S_0 = 1, S_1 = 1, S_2 = 1, S_3 = 1, S_4 = 1, S_5 = 0$). Lastly, the linear transformation applied to the input value (S_0) was

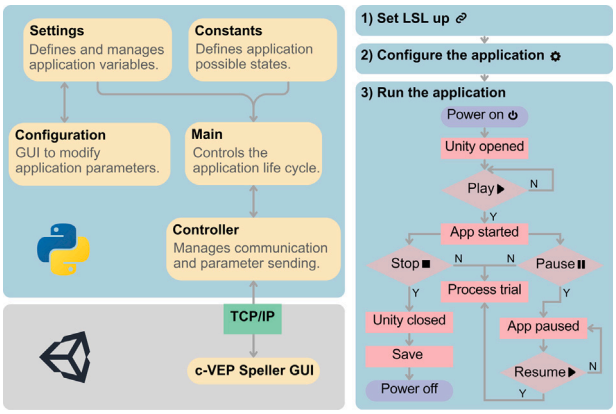

Fig. 1. Application architecture and workflow. *Left*: App components within MEDUSA©platform, their interactions, and communication with the GUI. *Right*: Application workflow showing required steps, user decision points (Y: Yes, N: No), and possible states. More information at https://docs.medusabci.com/.

performed through an XOR operation between the bits of the fifth (S_4) and sixth states (S_5). This transformation can be represented by the polynomial x^6+x^5+1. Once the m-sequence was generated, the circular shifting paradigm was used to obtain all possible temporally shifted versions of the sequence. Each of these versions, would subsequently encode different commands for the implemented c-VEP application [6].

2.4. App design

The c-VEP app used in this research is part of the MEDUSA© software ecosystem [24], a Python-based platform designed to facilitate and accelerate BCI development. From version 3.10 onward, the "c-VEP Speller" app, available on the MEDUSA© website (https://medusabci.com/market/cvep_speller/), includes the necessary features for adjusting opacity values and customizing background scenarios.

The main app components involved in the study were: (a) the background, which could be configured to display either a solid color or any image selected by the user from the file browser; (b) the command box, which appeared over the background and was black when the sequence bit was 0, and white when it was 1; and (c) the command character, which was positioned over the box and took either black or white, but in contrast to the box color to ensure visibility. Both the command box and character had adjustable opacity for each of their possible colors (black or white), resulting in four distinct opacity settings that could be customized from 0% to 100%, according to user preferences.

The graphical user interface was designed in Unity, primarily for two reasons: (i) it allows precise control over monitor refresh rates, which is essential in c-VEP to synchronize EEG signals with stimuli, and (ii) it provides a robust development environment for creating interactive applications. On the other hand, EEG signal processing was performed with Python, a programming language widely recognized for its flexibility and versatility in biomedical data processing. To implement the communication between Unity and Python, an asynchronous and bidirectional TCP/IP protocol was used. This communication was full-duplex, enabling simultaneous data transmission and reception at both ends of the communication channel. In the implemented c-VEP app, MEDUSA© functioned as the server, while Unity operated as the client. For a detailed view of the application architecture and workflow, refer to Fig. 1, which illustrates the components within MEDUSA© platform and their interactions, as well as the step-by-step process of the application workflow.

2.5. Evaluation protocol

All 10 users participating in the study followed a standardized evaluation protocol. The evaluation was conducted in a single session lasting 1 h. This session was divided into six sections (i.e., conditions), each featuring different opacity and background settings. To ensure a consistent progression, the conditions were presented in the same order for all participants, starting from higher opacity and gradually moving to lower opacity. This approach enabled direct comparisons between consecutive conditions, providing a clear reference point throughout the session. To minimize visual fatigue accumulation, participants were offered flexible breaks between conditions, allowing sufficient recovery time based on individual needs.

Each section included both training and testing phase. During the training phase, participants were instructed to observe a command that flickered according to the original m-sequence. A total of 3 recordings were made, with each recording consisting of 5 trials, and each trial containing 10 cycles, meaning by a cycle a complete repetition of the m-sequence. This resulted in a total of 150 cycles for training the model in each condition and for each user. The screen refresh rate was set to 120 Hz, yielding a cycle duration of 0.525 s (63 bits/120 Hz) and a total calibration time of 78.75 s.

In the testing phase, a 4×4 matrix was configured, consisting of 16 commands, corresponding to the letters "A" through "P" in alphabetical order. Each command had a lag of $\tau = 4$ bits. The number of cycles per selection was set at 10, resulting in a selection time of 5.25 s per command. Participants were instructed to make 16 selections in the exact order of the commands displayed. In the event of an incorrect selection, participants were instructed to proceed to the next command without attempting to correct the mistake.

The opacity and background settings were unique to each condition. The visual appearance of these settings is shown in Fig. 2, and the specific parameters for each condition are described as follows:

- **100 Plain Scenario (PS)**: All four opacity parameters set to 100%, with a uniform color background.
- **100 Realistic Scenario (RS)**: All four opacity parameters set to 100%, with a lifelike image as the background.
- **100/50**: Command box and character opacity set to 100% when the bit is 0 (black box, white character), and 50% when the bit is 1 (white box, black character), with a lifelike image as the background.
- **100/0**: Command box and character opacity set to 100% when the bit is 0, and 0% when the bit is 1, with a lifelike image as the background.
- **50/0**: Command box opacity set to 50% and character opacity set to 100% when the bit is 0; both set to 0% when the bit is 1, with a lifelike image as the background.
- **0/0**: Command box opacity set to 0% and character opacity set to 100% when the bit is 0; both set to 0% when the bit is 1, with a lifelike image as the background.

The tested conditions were carefully chosen to balance session duration and meaningful data collection. Pilot tests confirmed that three opacity levels (100%, 50%, and 0%) were sufficient to study the effects of opacity variation, with the impact of intermediate levels potentially extrapolated from these conditions. Additionally, the white box was made transparent while keeping the black box, as a prior study has shown that dark colors elicit greater amplitude brain responses in appearance–disappearance patterns [29]. The six selected conditions were deemed sufficient to analyze opacity effects while ensuring the session remained short enough to prevent participant discomfort.

The evaluation protocol also included the application of questionnaires to measure both the functionality of the application and the user experience. Two main questionnaires were conducted: one to assess visual fatigue and another to evaluate overall satisfaction. The visual

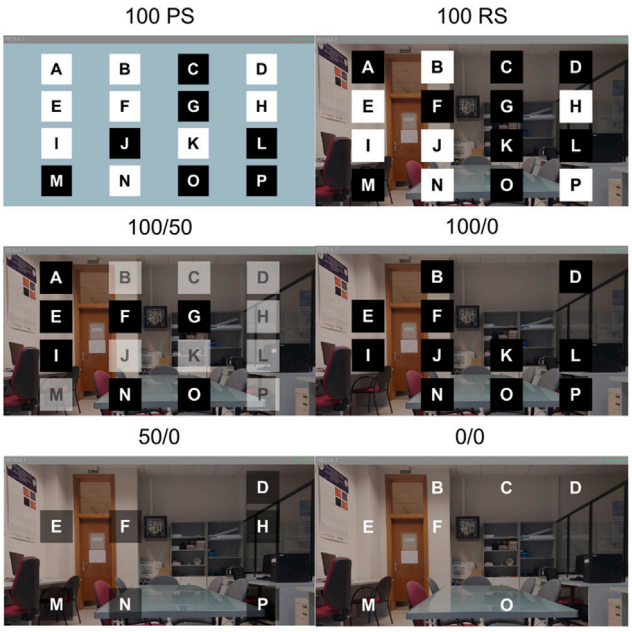

Fig. 2. Appearance of the application under the six experimental conditions (100 PS, 100 RS, 100/50, 100/0, 50/0, and 0/0), with variations in background (plain scenario or realistic scenario) and opacity settings (ranging from 0% to 100% for both black and white stimuli in both command box and character elements).

fatigue questionnaire was performed separately and in greater detail as evaluating visual fatigue is a key objective of the study. It is especially important considering that visual fatigue is a well-documented issue in c-VEP-based BCI and remains one of their major limitations [10]. In this questionnaire, users rated their level of fatigue at the end of each experimental condition on a scale from 0 (no visual fatigue) to 10 (extreme visual fatigue). The overall satisfaction questionnaire was designed to capture the broader user experience, as there are multiple factors beyond visual fatigue that influence the usability of the system. For instance, aspects such as user comfort – including the fit and feel of the EEG cap and the overall setup – the duration of the session, and the required concentration can significantly impact satisfaction [30]. This questionnaire was administered at the end of the session and included alternating positive and negative statements to control for acquiescence bias. Participants rated these statements on a Likert scale [31] ranging from 1 (strongly disagree) to 5 (strongly agree) and provided additional comments and suggestions through an open-ended question.

2.6. Signal processing

All EEG signals were pre-processed online using a notch filter at 50 Hz to eliminate network interference, along with a filter bank comprising three bandpass filters at the following frequencies: 1–60 Hz, 12–60 Hz, and 30–60 Hz [32]. All filters were of the infinite impulse response (IIR) Butterworth type and of order 7. Additionally, epochs with a standard deviation greater than three times the standard deviation of the other channels were rejected, as these epochs were considered to contain artifacts or noise.

For each filtered signal, further processing was performed using the reference c-VEP pipeline [6]. During calibration, the user observed a command encoded by the original m-sequence, repeated over a specific number of cycles. The initial EEG signal was reorganized by concatenating the individual cycles sequentially, resulting in a matrix with dimensions $k_c N_s \times N_c$, where k_c is the number of cycles, N_s the number of samples, and N_c the number of channels. Simultaneously, the signal was divided into epochs corresponding to a full cycle to compute the average, producing a signal with dimensions $N_s \times N_c$, which was replicated k_c times to match the dimensions of the first signal [6]. Averaging enhances the event-related potential (ERP) components since individual epochs are often highly contaminated by noise. By averaging, the non-task-related components (i.e., noise) are reduced due to their random nature, allowing the event-related components to be amplified.

Once the two signals, concatenated (A) and averaged (B), were obtained, they were introduced into a canonical correlation analysis (CCA) function [33]. The objective of this function is to find the coefficients that, when multiplied to the signals, maximize their correlation. This process is described by the following equation:

$$\max_{W_a, W_b} \frac{W_a^T A^T B W_b}{\sqrt{W_a^T A^T A W_a \cdot W_b^T B^T B W_b}}. \quad (1)$$

From the coefficient matrices W_a and W_b returned by Eq. (1), only the first component of W_b (i.e., the first column), denoted as w_b, was taken. This component, with dimensions $N_c \times 1$, acts as a spatial filter that weighs the importance of each channel when creating the template. The signal B was projected onto this vector, generating a template of dimensions $N_s \times 1$ that represents the user response to the original m-sequence. Additionally, by circularly shifting a specified number of samples (τ), all possible templates for the displaced versions of the m-sequence were created. In total, $M \times 3$ templates were obtained, where M represent the number of available commands and 3 corresponds to the number of filters that comprised the filter bank [6].

During the testing phase, the EEG signal was recorded while the user focused on an unknown command, with the goal of identifying it. The recorded signal was pre-processed the same way it was during calibration, with each filtered signal from the filter bank divided into epochs corresponding to selection cycles. Epoch averaging was performed, and the resulting signal was projected using w_b. The projection was then compared to all templates generated during calibration using Pearson correlation. Finally, the command with the highest average correlation across the filter bank was selected as the predicted command [6].

3. Results

3.1. Accuracy

The accuracy analysis involved examining the results of the spelling task completed by users under each condition. Detailed results for 10 selection cycles are presented in Table 1. In addition, for each participant and condition, the analysis assessed the outcome of each cycle against the target labels, calculating accuracy per cycle, user and condition. The average accuracies across participants for the six conditions were then computed, and an accuracy curve was plotted for each condition, as shown in Fig. 3. The full set of unfolded accuracy results for each selection cycle, user, and condition is provided in the supplementary material.

Statistical analysis was performed using the Wilcoxon signed-rank test to conduct pairwise comparisons between conditions, with differences assessed across 10 selection cycles. To control for the false discovery rate (FDR), the Benjamini–Hochberg method was employed. The results indicated statistically significant differences (p-value < 0.05) in accuracy between the 100 PS, 100 RS, and 100/50 conditions compared to the 100/0, 50/0, and 0/0 conditions. Detailed p-values for all pairwise comparisons are illustrated in the upper triangle of the matrix in Fig. 4. Additional results from the statistical analysis at cycle level can be found in the supplementary material.

3.2. Spatial filters

The vector w_b obtained from CCA serves as a spatial filter, applying weights to the signal from each EEG channel. The highest absolute magnitude values in w_b are those that most significantly contribute to

Table 1
Accuracy (%) with 10 selection cycles for each condition and user.

User	100 PS	100 RS	100/50	100/0	50/0	0/0
U01	100.00	100.00	100.00	100.00	100.00	93.75
U02	100.00	100.00	100.00	93.75	93.75	93.75
U03	100.00	100.00	100.00	100.00	93.75	68.75
U04	100.00	100.00	100.00	68.75	68.75	62.50
U05	100.00	100.00	100.00	93.75	87.50	87.50
U06	100.00	100.00	100.00	62.50	50.00	56.25
U07	100.00	100.00	93.75	43.75	87.50	87.50
U08	100.00	100.00	100.00	93.75	100.00	81.25
U09	100.00	100.00	100.00	93.75	93.75	87.50
U10	100.00	100.00	100.00	100.00	100.00	100.00
Mean	**100.00**	**100.00**	**99.38**	**85.00**	**87.50**	**81.88**
SD[a]	**0.00**	**0.00**	**1.88**	**18.58**	**15.31**	**13.82**

[a] SD: standard deviation.

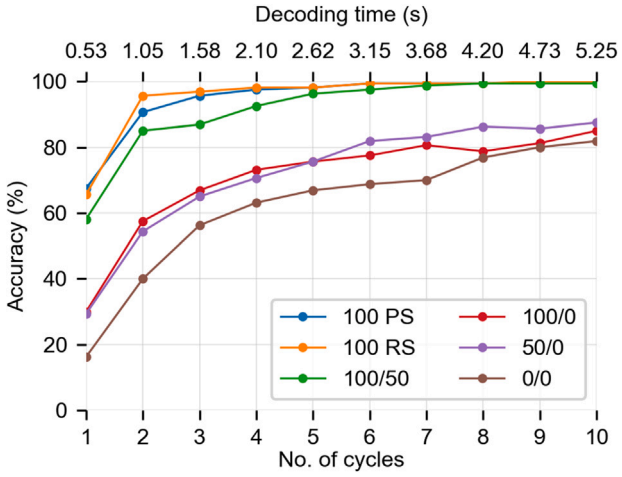

Fig. 3. Average accuracy curves per selection cycle for each of the six experimental conditions. The lower x-axis represents the cycle number, while the upper x-axis indicates the decoding time in seconds for each cycle.

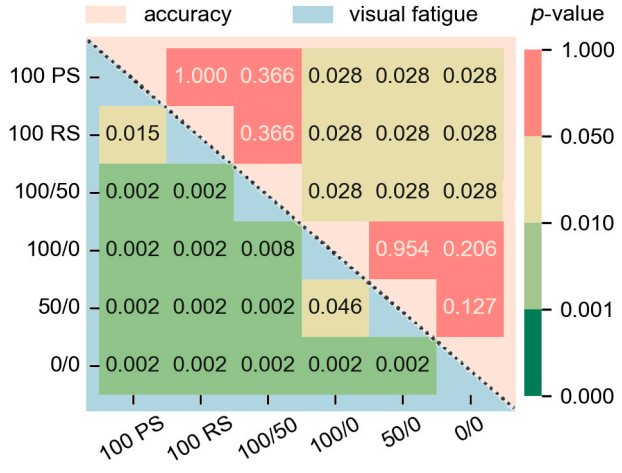

Fig. 4. Matrix of p-values obtained from statistical analyses using the Wilcoxon signed-rank test and Benjamini–Hochberg for FDR control. The upper triangle of the matrix displays results from the accuracy analysis, while the lower triangle presents results from the visual fatigue analysis.

maximizing the correlation between the ERP derived from averaging multiple cycles and the concatenated signal containing a single epoch. When projecting the signal of $N_s \times N_c$ dimensions onto this vector

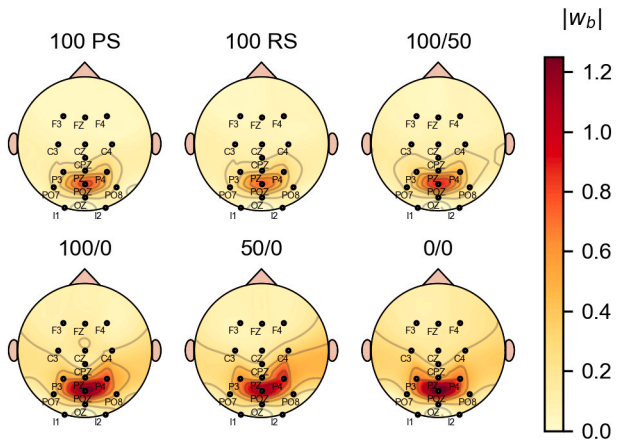

Fig. 5. Grand-averaged topographic plots from the spatial filters ($|w_b|$) derived from calibration for each condition.

with dimensions $N_c \times 1$, the channels with higher importance for VEP formation will receive a higher weighting.

To analyze this spatial filter, the vector w_b was visualized using average topographic plots across participants, with one plot created for each condition. First, w_b values were transformed to their absolute values. Next, the maximum value from all filters was used to standardize the visualization scale across conditions. The resulting topographies, shown in Fig. 5, illustrate the spatial distribution of the w_b weight vector on the scalp, with electrodes represented as points based on their locations, and data interpolated for a continuous representation. Topographic plots for each user and condition are available in the supplementary material.

3.3. Brain responses

EEG data analysis involved computing brain response signals for each condition using calibration recordings (150 cycles per condition and user). In the time domain, epochs were averaged across users and cycles to derive a grand-averaged brain response per condition. The resulting signals were visualized in the POz and Oz channels due to their proximity to the primary visual cortex, where VEP formation occurs [34,35]. For time–frequency domain analysis, spectrograms were computed for each epoch using 250 ms windows with 93.75% overlap and 256 FFT points. These spectrograms were then averaged across cycles and users to obtain a single spectrogram per condition. Only the POz channel was used in this and subsequent analyses, as it showed stronger activation in trained spatial filters than Oz. The frequency range was restricted to 4–30 Hz, determined by the 250 ms windowing (which set the 4 Hz lower limit) and minimal activity above 30 Hz. Both time-amplitude and time–frequency analyses are presented in Fig. 6(a).

Subsequently, comparisons between conditions were conducted using dynamic time warping (DTW) [36] and correlation analysis. DTW is a time-series algorithm that measures similarity between temporal sequences by finding an optimal alignment. It accommodates variations in sequence length and temporal shifts by adjusting the time axis, making it especially useful for EEG analysis [37], where latency shifts can occur. In this study, DTW was employed to identify characteristic alignment patterns between conditions, which may reflect consistent components across different brain responses. To ensure reliable comparisons, conditions were grouped into (1) 100 PS, 100 RS, 100/50 and (2) 100/0, 50/0, 0/0, avoiding inconsistencies in the transition from 100/50 to 100/0. The resulting alignment paths, shown in Fig. 6(b), illustrate how responses in one condition adjusted to another. Next, a correlation analysis was performed to quantify the similarity

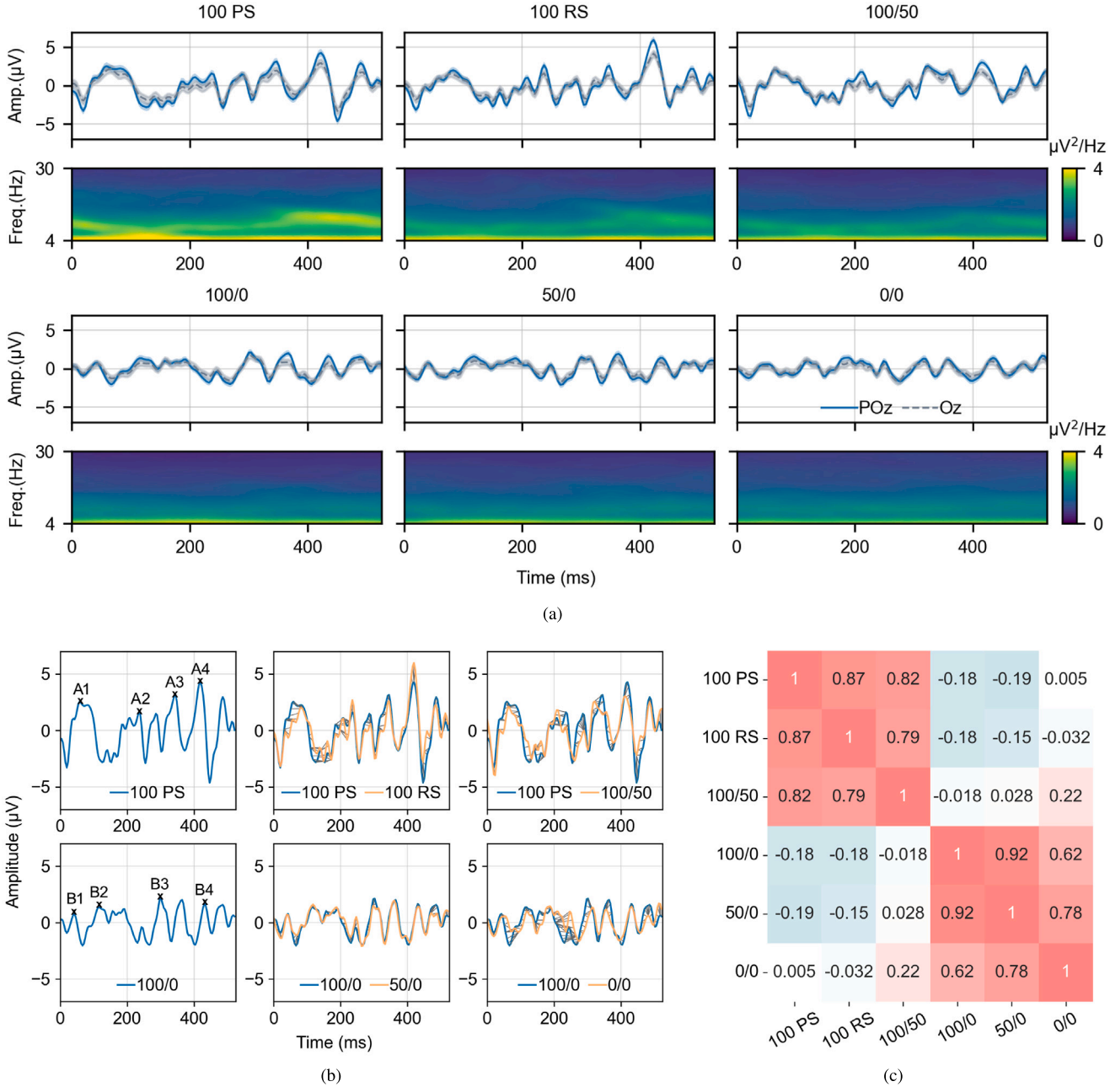

Fig. 6. (a) *Top*: Grand average of calibration epochs across users for each condition at the POz (continuous blue line) and Oz (dashed gray line) channels. Lines showing mean and shaded regions 95% confidence interval. *Bottom*: Grand average spectrograms of calibration epochs across users for each condition at POz. (b) DTW alignment paths, reference signal at POz (blue) matched with the conditions under comparison at POz (orange). Four representative peaks, selected as examples of consistent components across groups of conditions, are labeled. (c) Correlation matrix among all grand-averaged brain responses at POz.

between brain responses across conditions. Spearman correlation metric was chosen since linear relationships among conditions could not be assumed. The resulting correlation matrix is displayed in Fig. 6(c).

Finally, to further investigate key components of the visual response, four peaks per group were selected based on DTW findings and a relatively even temporal distribution. Peaks in the first group were labeled A1–A4, while those in the second group were labeled B1–B4. These peaks are marked in Fig. 6(b), with their amplitude and latency values summarized in Table 2.

Brain responses at individual level, DTW alignment paths relative to each condition and the DTW-based distance matrix are available at the supplementary material.

3.4. Questionnaires

The results from the questionnaires completed by users were collected and analyzed. Individual scores were averaged to obtain a mean visual fatigue score for each condition, along with mean scores for each item on the overall satisfaction questionnaire. The mean visual fatigue scores, rated on a scale from 0 (none) to 10 (extreme), for the conditions 100 PS, 100 RS, 100/50, 100/0, 50/0, and 0/0 were 6.4, 5.5, 3.7, 2.8, 2.4, and 1.1, respectively. Fig. 7 displays a boxplot illustrating the distribution of scores for each condition. For the satisfaction questionnaires, the mean scores and standard deviations for each item are summarized in Table 3. Additionally, individual user responses can be found at the supplementary material.

Table 2
Amplitude (μV) and latency (ms) of selected peaks (A1–A4, B1–B4) across different conditions.

		100 PS	100 RS	100/50			100/0	50/0	0/0
A1	Latency (ms)	59	82	62	B1	Latency (ms)	43	39	51
	Amplitude (μV)	2.55	2.02	2.07		Amplitude (μV)	0.75	0.72	0.57
A2	Latency (ms)	234	234	211	B2	Latency (ms)	117	117	117
	Amplitude (μV)	1.60	2.68	1.79		Amplitude (μV)	1.36	1.60	0.99
A3	Latency (ms)	344	344	320	B3	Latency (ms)	301	297	312
	Amplitude (μV)	3.15	2.61	2.57		Amplitude (μV)	2.13	1.50	1.31
A4	Latency (ms)	418	418	410	B4	Latency (ms)	430	430	430
	Amplitude (μV)	4.28	5.98	3.04		Amplitude (μV)	1.65	1.42	1.41

Table 3
Mean scores and standard deviations of satisfaction questionnaire items on a Likert scale (1: strongly disagree, 5: strongly agree).

Item	Mean	SD[a]
The session duration was adequate.	4.8	0.4
I had difficulty maintaining my concentration during the session.	1.9	0.8
The system is intuitive and easy to use.	4.7	0.6
I experienced discomfort during the session.	1.7	0.8
By varying opacity I have noticed significant changes in visual comfort and eyestrain.	4.3	0.8
In general, the system has not responded in accordance with my intentions.	1.7	0.6
I consider that the system could be useful in extended reality scenarios.	4.7	0.5

[a] SD: standard deviation.

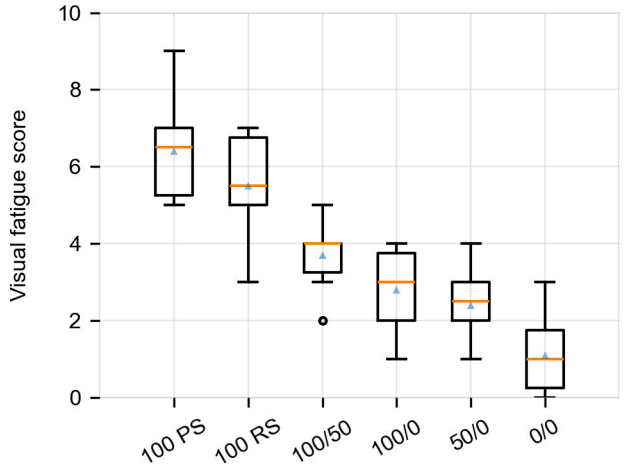

Fig. 7. Score from 0 (none) to 10 (extreme) of visual fatigue experienced by users.

Statistical comparisons were conducted on the visual fatigue scores for each condition. Pairwise comparisons were performed using the Wilcoxon signed-rank test, with the Benjamini–Hochberg method applied to control for the FDR. This analysis revealed statistically significant differences (p-value < 0.05) across all pairwise comparisons. Detailed p-values for these comparisons are presented in the lower triangle of the matrix in Fig. 4.

4. Discussion

4.1. Stimulus opacity and c-VEP decoding performance

The first research question addressed in this study was to investigate the relationship between visual stimulus opacity and c-VEP decoding performance. The accuracy results from the evaluation protocol, presented in Table 1, provide valuable insights into this relationship. The results indicate that changing the background over which the commands are visualized does not impact accuracy, as both the 100 PS and 100 RS conditions consistently yielded 100% average accuracy. However, reducing the opacity of the visual stimuli resulted in statistically significant variations in accuracy, as shown by the p-values in Fig. 4. For instance, in the 100/50 condition, average accuracy remained high at 99.38%, but as opacity was further reduced – with the white color being made completely transparent in the 100/0 condition – average accuracies dropped to 85.00%, 87.50%, and 81.88% for the 100/0, 50/0, and 0/0 conditions, respectively.

While the overall accuracy for 10 selection cycles is noteworthy, further analysis reveals additional details. For the 100/0 condition, 7 out of 10 participants maintained accuracies equal to or above 93.75%. When considering the median, which is less influenced by outliers, the accuracy for this condition reaches 93.75%, underscoring that the majority of participants were only mildly affected by the change in opacity. However, a subset of participants experienced a sharp decline in performance from 100/50 to 100/0. This suggests that while most users can tolerate some reduction in stimulus opacity without a substantial impact on performance, a minority are highly sensitive to such changes. One notable outlier was participant U07, who exhibited poor accuracy for the 100/0 condition but then showed significant improvement for the 50/0 and 0/0 conditions. This unexpected result, where accuracy improved under conditions that would be expected to perform worse, suggests that individual variability or external factors (i.e., attention loss, tiredness, etc.) may have influenced performance during this specific condition.

An additional finding of interest concerns the accuracy curves over selection cycles and time shown in Fig. 3. For the conditions 100 PS, 100 RS, and 100/50, the accuracy curves plateaued after a few selection cycles, indicating that optimal performance was reached quickly. However, for the 100/0, 50/0, and 0/0 conditions, the accuracy curves grew more slowly and had not plateaued after 10 selection cycles, suggesting that performance might improve with longer selection times. This indicates that while reducing stimulus opacity negatively impacts short-term accuracy, extending the selection time could mitigate these effects and allow for improved performance.

Despite the considerable decline in average performance from 100/50 to 100/0, the accuracy results across all six conditions remain optimal for BCI control and are comparable to the performance of other c-VEP-based BCI spellers reported in the literature. For instance, Gembler et al. (2019) [38] achieved 95.9% accuracy with their c-VEP-based spelling system, Nagel et al. (2019) [39] reported an accuracy of 98.2% in their keyboard system for healthy participants, and Verbaarschot et al. (2021) [40] demonstrated c-VEP-based communication systems for ALS patients, with accuracy rates ranging from 79.3% to 94.3%, depending on the group. Furthermore, a similar drop in accuracy when one of the two flickering stimuli is made transparent was previously

observed by Liu et al. (2024) [22] using SSVEP. In that case, accuracy decreased from 86.17% to less than 80%.

To gain a more comprehensive understanding of the relationship between stimulus opacity and c-VEP performance, it is important to go beyond analyzing accuracy alone. Additional analyses, particularly those focused on spatial filters obtained from CCA and EEG data, provide deeper insights into how opacity influences the decoding of c-VEP. Regarding spatial filter analysis, the topographic plots in Fig. 5 indicate that the parieto-occipital region remains the most relevant across all conditions, with the highest absolute values for w_b around POz. However, there is a slight increase in the absolute weights of electrodes in this region for the last conditions compared to the first, which may hint at a connection to the observed decrease in performance.

The EEG analysis presented in Fig. 6 reveals that the significant drop in accuracy between the 100/50 and 100/0 conditions is linked to changes in the morphology of the brain response signals obtained from averaging calibration epochs in the POz and Oz channels. As shown in Fig. 6(a), the brain responses for the first three conditions (100 PS, 100 RS, and 100/50) exhibit similar patterns, while those for the last three conditions (100/0, 50/0, and 0/0) diverge considerably. This divergence is further confirmed by the correlation analysis, which indicates strong correlations among the first three conditions and among the last three, but minimal correlation between any of the first three and any of the last three, as illustrated in the correlation matrix in Fig. 6(c). Additionally, the DTW analysis reinforces this distinction, clearly separating the first three conditions from the last three. When grouped into these two sets, components of the different brain responses align well, as shown in 6(b). However, aligning a condition from the first group with one from the second proves more challenging (see supplementary material for more details). This suggests that visual response components are not necessarily related when opacity conditions are altered.

The time–frequency domain analysis shows that most brain activity occurs within the 4–30 Hz range, with minimal power detected above 30 Hz. The 100 PS condition exhibits the highest spectral power, peaking around 400 ms in the 10–15 Hz range, a trend also observed in the 100 RS condition and, to a lesser extent, in the 100/50 condition. However, this pattern is absent in other conditions. In general, the time–frequency domain analysis offers limited insights, with no clear relationship to opacity adjustment.

When examining the peak characteristics identified and analyzed for each group of conditions (Table 2), it can be said that the A peaks exhibit greater variability in both latency and amplitude across the different conditions compared to the B peaks. Moreover, the amplitudes of the A peaks are generally greater than those of the B peaks. In the first set of conditions, both the latency and amplitude of all peaks tend to decrease for the 100/50 condition. In the second set of conditions, latencies remain consistent, except for B1, while amplitudes generally decrease as the conditions transition to more transparent stimulation. It is important to consider that these peaks are not components of the VEP itself, but rather represent features of the observed brain responses. Given the nature of c-VEP, it is not possible to extract an isolated VEP; rapid stimulus alternation leads to overlapping responses, and studies have shown that nonlinear interactions play a significant role in shaping c-VEP responses [6].

Synthesizing the information extracted from the EEG analysis, it can be stated that there is a notable change in the brain visual response when transitioning from 100/50 to 100/0, but not when going from 100/100 to 100/50. These findings suggest that incorporating some transparency into the stimuli may have a smaller impact on the brain response than initially expected, provided that the black-white contrast is preserved. In the 100/0 condition, it is important to note that one of the two stimuli is effectively absent, resulting in a flickering effect that appears black-transparent. This resembles appearance–disappearance stimulation rather than pattern reversal [29]. Unlike the white-black flickering that offers maximum contrast and yields the highest VEP amplitude [41], the absence of one stimulus in the 100/0 condition reduces overall contrast. This diminished contrast leads to a lower amplitude brain response, as there is a relationship between the neural mechanisms responsible for processing visual stimuli and stimulus contrast [41,42]. Indeed, A peaks are no longer identifiable under black-transparent stimulation conditions. This suggests that the change in visual response is significant enough to alter the signal components, preventing DTW analysis from aligning the same peaks across all conditions when determining optimal sequence alignment paths.

4.2. Stimulus opacity and user experience

The second research question focused on user experience and the impact of visual stimuli, particularly concerning visual fatigue experienced by users. As shown in Fig. 7, visual fatigue significantly decreased as users progressed to settings with greater transparency. However, transparency alone was not the only factor contributing to this reduction; transitioning from a plain background to a realistic scenario also enhanced user experience. This improvement is evident when comparing the scores between the 100 PS and 100 RS conditions, where a statistically significant decline in user ratings was observed. This finding underscores the potential for integrating c-VEP into XR environments, as it aligns with previous BCI-XR studies indicating that immersive experiences enhance user engagement, motivation, and overall experience [30,43].

Fig. 4 highlights the statistically significant reductions in visual fatigue as opacity is reduced, with all proposed conditions achieving p-values < 0.05 when compared to either the initial or any preceding conditions. The most notable reduction occurred when transitioning from the 100 RS condition to the 100/50 condition, where the mean score dropped from 5.5 to 3.7—a decrease of 1.8 points. Interestingly, an inverse relationship was observed between user comfort and accuracy: enhancing user experience led to a decrease in accuracy, and vice versa. For instance, while the 0/0 condition resulted in the lowest visual fatigue score, approaching zero, it also produced the lowest accuracy. To balance these two aspects, the 100/50 condition is suggested, as it achieved 99.38% accuracy while significantly reducing visual fatigue, with scores nearly halved compared to the 100 PS condition. It is important to note that the nature of the evaluation protocol may have introduced potential bias due to the order in which conditions were presented, particularly in terms of accumulated visual fatigue. However, it is observed that participants reported lower fatigue scores for conditions completed later in the study. This suggests that the order of conditions did not introduce bias against our hypothesis and may have, in fact, reinforced the findings.

Other scientific approaches have also successfully reduced visual fatigue by implementing various changes in the c-VEP paradigm. As noted in the introduction, successful strategies have included using pseudo-random sequences that concentrate power in higher frequencies [9,14], employing non-binary sequences [13,16], and presenting visual stimuli in a checkerboard pattern [17]. Visual fatigue scores from these studies have been standardized to a 0 to 10 scale for comparison. This comparison consisted of the difference between the score of the condition evaluated as reference, and the score of the condition that caused the least visual fatigue for the users. For this analysis, only the 100 PS, 100 RS, and 100/50 conditions will be considered, as the others showed a statistically significant decrease in accuracy. Table 4 presents the results of this comparison, showing that changes in visual stimulus opacity achieved a significant improvement in visual fatigue, even surpassing other strategies aimed at optimizing the c-VEP paradigm to enhance user accessibility. Perhaps some of these strategies could be combined to further enhance user comfort while maximizing system performance.

Further insights were gained from the satisfaction questionnaires, as presented in Table 3. The system was perceived as intuitive and easy to use, with no notable discomfort experienced during the session.

Table 4
Comparison of user-reported visual fatigue scores across different studies approaching modifications to the c-VEP paradigm.

Study	Reference condition[a]	Score (0-10)[c]	Suggested condition[b]	Score (0-10)[c]	Difference
Shirzhiyan et al. 2019 [14]	mseq	5.90	chaotic codes	4.80	1.10
Gembler et al. 2020 [16]	binary	5.00	quintary	3.60	1.40
Martínez-Cagigal et al. 2023 [13]	GF(2^6)	6.00	GF(7^2)	4.00	2.00
Fernández-Rodríguez et al. 2023 [17]	C001	4.50	C016	3.50	1.00
Cabrera Castillos et al. 2023 [9]	mseq 40	4.75	burst 40	3.00	1.75
Current study	**100 PS**	**6.40**	**100/50**	**3.70**	**2.70**

[a] Reference condition used for comparison.
[b] Condition with best results in terms of visual fatigue score.
[c] Scores have been standardized to a 0–10 scale for comparability across studies.

Users also felt that the system adequately responded to their intentions, reinforcing the positive impact of the design. Most importantly, variations in stimulus opacity resulted in significant improvements in user experience, further demonstrating the value of this adjustment. Notably, all users expressed that the application of c-VEP could be beneficial in XR scenarios.

4.3. Main contributions

This study makes significant contributions to the field of c-VEP-based BCI by introducing the analysis of visual stimulus opacity, a previously unexplored factor. This innovation not only advances the design of more comfortable BCI but also enables the integration of these systems into lifelike environments, expanding their potential applications. The study comprehensively covers all stages of an experimental investigation: design, implementation, validation, and result extraction, providing an in-depth perspective on the topic. Additionally, a thorough analysis of several conditions was conducted, offering a detailed understanding of how opacity in visual stimuli affects c-VEP performance. These efforts lead to valuable insights that could drive the advancement of c-VEP-based BCI, particularly in terms of enhancing user experience.

4.4. Limitations and future work

The present study is noteworthy for its innovative approach; however, several limitations must be acknowledged. The relatively small and homogeneous sample size, consisting exclusively of healthy young individuals, restricts the generalization of the findings. To enhance the robustness of future research, it would be interesting to increase the sample size and include a more diverse pool of participants, particularly individuals with motor disabilities.

Additionally, investigating a broader range of conditions, such as reverse opacity settings (50/100, 0/100, 0/50), or incorporating additional opacity levels (25% and 75%), could offer valuable insights into the relationship between stimulus opacity, user experience, and system performance. Studying individual performance variability among users will be useful, particularly in characterizing those who are more susceptible to changes in opacity. Moreover, incorporating single VEP measurements for each experimental condition could help overcome the challenges posed by superimposed stimuli in c-VEP brain response analysis.

Furthermore, incorporating advanced techniques such as deep learning methods for signal processing, could improve the identification of complex patterns in brain activity, thereby enhancing system performance. Future research should also consider incorporating eye-tracking technology to offer objective measurements of visual fatigue, providing a more reliable understanding of user experience. Finally, exploring the integration of c-VEP applications into various XR scenarios would enable a more realistic evaluation of these systems in lifelike environments. Addressing these limitations could lead to more effective applications of c-VEP-based BCI research.

5. Conclusion

In this study, a comprehensive and novel investigation was conducted to assess the impact of stimulus opacity on both system accuracy and user experience in c-VEP-based BCI. The traditional paradigm was modified by progressively reducing the opacity of visual stimuli, allowing commands to blend more seamlessly into lifelike environments. Six opacity combinations were tested with 10 healthy participants, yielding valuable insights into the interplay between system performance and user experience.

Reducing opacity has been shown to enhance user experience by minimizing visual fatigue, although it may impact system accuracy. Significant differences emerged when transitioning from black and white to black and transparent stimulation, affecting both accuracy and brain responses. A balanced outcome was achieved with 50% white opacity and 100% black opacity, resulting in 99.38% accuracy and a visual fatigue score of 3.7/10. Under this condition, statistically significant differences were observed in visual fatigue scores; however, no significant differences in accuracy were detected compared to traditional black and white stimuli at 100% opacity.

To summarize, the study presents important findings regarding the key research questions. On one hand, there is a relationship between c-VEP performance and stimulus opacity. Reducing opacity does not decrease average accuracy as long as black and white contrast is maintained; however, accuracy declines when one color becomes completely transparent. This decline is also associated with changes in the brain response signal. On the other hand, reducing the visual stimulus opacity enhances the user experience by significantly reducing visual fatigue. Furthermore, the introduction of partial transparency in visual stimuli facilitates the integration of c-VEP-based BCI into lifelike environments, supporting their use in immersive settings.

CRediT authorship contribution statement

Ana Martín-Fernández: Writing – original draft, Validation, Software, Methodology, Formal analysis, Data curation, Conceptualization. **Víctor Martínez-Cagigal:** Writing – review & editing, Supervision, Software, Methodology, Conceptualization. **Selene Moreno-Calderón:** Writing – review & editing, Supervision, Methodology. **Eduardo Santamaría-Vázquez:** Writing – review & editing, Supervision, Software. **Roberto Hornero:** Writing – review & editing, Supervision, Funding acquisition.

Declaration of competing interest

There is no conflict of interest.

Acknowledgments

This work was supported by the project 0124_EUROAGE_MAS_4_E, cofunded by the European Union through the Interreg VI-A Spain-Portugal Program (POCTEP) 2021–2027. This publication is part of the TED2021-129915B-I00 action, funded by MICIU/AEI /10.13039/501100011033 and the European Union NextGenerationEU/ PRTR.

This work was supported by the Regional Goverment of Castilla y León (Junta de Castilla y León, Consejería de Educación) and the EU-FEDER under the project VA140P24. This work was supported by "Centro de Investigación Biomédica en Bioingeniería, Biomateriales y Nanomedicina (CIBER-BBN)" through "Instituto de Salud Carlos III" co-funded with ERDF funds.

Appendix A. Supplementary data

Supplementary material related to this article can be found online at https://doi.org/10.1016/j.bspc.2025.107894.

Data availability

Data will be made available on request.

References

[1] J. Wolpaw, E.W. Wolpaw, Brain–Computer Interfaces: Principles and Practice, Oxford University Press, 2012.
[2] E. López-Larraz, et al., Brain-machine interfaces for rehabilitation in stroke: a review, NeuroRehabilitation 43 (2018) 77–97.
[3] S. Moreno-Calderón, et al., Combining brain-computer interfaces and multiplayer video games: an application based on c-VEPs, Front. Hum. Neurosci. 17 (2023).
[4] E. Yin, et al., A dynamically optimized SSVEP brain–computer interface (BCI) speller, IEEE Trans. Biomed. Eng. 62 (2014) 1447–1456.
[5] B.-K. Min, et al., Neuroimaging-based approaches in the brain–computer interface, Trends Biotechnol. 28 (2010) 552–560.
[6] V. Martínez-Cagigal, et al., Brain–computer interfaces based on code-modulated visual evoked potentials (c-VEP): a literature review, J. Neural Eng. 18 (2021) 061002.
[7] M. Spüler, et al., Online adaptation of a c-VEP brain-computer interface (BCI) based on error-related potentials and unsupervised learning, PloS One 7 (2012) e51077.
[8] F. Gembler, et al., Dynamic time window mechanism for time synchronous VEP-based BCIs—performance evaluation with a dictionary-supported BCI speller employing SSVEP and c-VEP, PloS One 14 (2019) e0218177.
[9] K.C. Castillos, et al., Burst c-VEP based BCI: Optimizing stimulus design for enhanced classification with minimal calibration data and improved user experience, NeuroImage 284 (2023) 120446.
[10] C.P. Gentile, G.K. Aguirre, A neural correlate of visual discomfort from flicker, J. Vis. 20 (2020) 11.
[11] F. Gembler, et al., Effects of monitor refresh rates on c-VEP BCIs, in: Symbiotic Interaction: 6th International Workshop Symbiotic 2017, Eindhoven, The Netherlands, December 18–19, 2017, Revised Selected Papers 6, Springer, 2018, pp. 53–62.
[12] T. Başaklar, et al., Effects of high stimulus presentation rate on EEG template characteristics and performance of c-VEP based BCIs, Biomed. Phys. Eng. Express 5 (2019) 035023.
[13] V. Martínez-Cagigal, et al., Non-binary m-sequences for more comfortable brain–computer interfaces based on c-VEPs, Expert Syst. Appl. 232 (2023) 120815.
[14] Z. Shirzhiyan, et al., Introducing chaotic codes for the modulation of code modulated visual evoked potentials (c-VEP) in normal adults for visual fatigue reduction, PLoS One 14 (2019) e0213197.
[15] E. Lai, et al., High-frequency discrete-interval binary sequence in asynchronous C-VEP-based BCI for visual fatigue reduction, IEEE J. Biomed. Heal. Informatics 28 (2024) 2769–2780.
[16] F.W. Gembler, et al., Five shades of grey: exploring quintary m-sequences for more user-friendly c-VEP-based BCIs, Comput. Intell. Neurosci.: CIN 2020 (2020).
[17] Á. Fernández-Rodríguez, et al., Influence of spatial frequency in visual stimuli for cVEP-based BCIs: evaluation of performance and user experience, Front. Hum. Neurosci. 17 (2023).
[18] S. Park, et al., Development of an online home appliance control system using augmented reality and an SSVEP-based brain–computer interface, IEEE Access 7 (2019).
[19] F. Wang, et al., A portable SSVEP-BCI system for rehabilitation exoskeleton in augmented reality environment, Biomed. Signal Process. Control. 83 (2023) 104664.
[20] Y. Du, X. Zhao, Visual stimulus color effect on SSVEP-BCI in augmented reality, Biomed. Signal Process. Control. 78 (2022) 103906.
[21] S.R. Zehra, et al., Evaluation of optimal stimuli for SSVEP-based augmented reality brain-computer interfaces, IEEE Access 11 (2023) 87305–87315.
[22] H. Liu, et al., A comparative study of stereo-dependent SSVEP targets and their impact on VR-BCI performance, Front. Neurosci. 18 (2024) 1367932.
[23] R. Oostenveld, P. Praamstra, The five percent electrode system for high-resolution EEG and ERP measurements, Clin. Neurophysiol. 112 (2001) 713–719.
[24] E. Santamaría-Vázquez, et al., MEDUSA©: A novel python-based software ecosystem to accelerate brain-computer interface and cognitive neuroscience research, Comput. Methods Programs Biomed. 230 (2023) 107357.
[25] Christian Kothe, et al., The lab streaming layer for synchronized multimodal recording, bioRxiv [Preprint] (2024) 580071.
[26] W. Park, J. Komo, The autocorrelation of m-sequences over nonprime finite fields, IEEE Trans. Aerosp. Electron. Syst. 24 (1988) 459–461.
[27] A. Ahmad, et al., Computing and listing of number of possible m-sequence generators of order n, Indian J. Sci. Technol. 6 (2013) 5359–5369.
[28] T.W. Cusick, P. Stănică, Chapter 2 - fourier analysis of boolean functions, in: T.W. Cusick, P. Stănică (Eds.), Cryptographic Boolean Functions and Applications, Academic Press, Boston, 2009, pp. 5–24.
[29] V. Zemon, J. Gordon, Luminance-contrast mechanisms in humans: visual evoked potentials and a nonlinear model, Vis. Res. 46 (2006) 4163–4180.
[30] H. Pan, et al., Comprehensive evaluation methods for translating BCI into practical applications: usability, user satisfaction and usage of online BCI systems, Front. Hum. Neurosci. 18 (2024) 1429130.
[31] R. Likert, A technique for the measurement of attitudes, Arch. Psychol. (1932).
[32] F.W. Gembler, et al., Asynchronous c-VEP communication tools—efficiency comparison of low-target, multi-target and dictionary-assisted BCI spellers, Sci. Rep. 10 (2020) 17064.
[33] W.K. Härdle, et al., Canonical correlation analysis, Appl. Multivar. Stat. Anal. (2015) 443–454.
[34] D.L. Clark, et al., The Brain and Behavior: An Introduction to Behavioral Neuroanatomy, Cambridge University Press, 2010.
[35] D.J. Creel, Visually evoked potentials, Handb. Clin. Neurol. 160 (2019) 501–522.
[36] M. Müller, Dynamic Time Warping, Springer Berlin Heidelberg, 2007, pp. 69–84.
[37] H.-C. Huang, B. Jansen, EEG waveform analysis by means of dynamic time-warping, Int. J. Bio-Med. Comput. 17 (1985) 135–144.
[38] F. Gembler, I. Volosyak, A novel dictionary-driven mental spelling application based on code-modulated visual evoked potentials, Computers 8 (2019) 33.
[39] S. Nagel, M. Spüler, Asynchronous non-invasive high-speed BCI speller with robust non-control state detection, Sci. Rep. 9 (2019) 8269.
[40] C. Verbaarschot, et al., A visual brain-computer interface as communication aid for patients with amyotrophic lateral sclerosis, Clin. Neurophysiol. 132 (2021) 2404–2415.
[41] M. Zaletel, et al., Effects of visual contrast on visual evoked potentials and doppler signal, Eur. J. Neurosci. 19 (2004) 3353–3358.
[42] F. Campbell, L. Maffei, Electrophysiological evidence for the existence of orientation and size detectors in the human visual system, J. Physiol. 207 (1970) 635.
[43] A. Alhakamy, Extended reality (XR) toward building immersive solutions: The key to unlocking industry 4.0, ACM Comput. Surv. 56 (2024) 1–38.